Circular RNA_0000326 accelerates breast cancer development via modulation of the miR-9-3p/YAP1 axis

Xiao-Ling XUE[1,#], Shuai ZHAO[2,#], Meng-Chang XU[3], Ying LI[4], Wen-Fei LIU[5], Hong-Zhen QIN[5,*]

[1]Radiology Department, Fujian Maternity and Child Health Hospital, Affiliated Hospital of Fujian Medical University, Fuzhou 350001, Fujian Province, China; [2]Breast Surgery Department, Fujian Maternity and Child Health Hospital, Affiliated Hospital of Fujian Medical University, Fuzhou 350001, Fujian Province, China; [3]Academician Workstation, Changsha Medical University, Changsha 410219, Hunan Province, China; [4]Senior Department of Oncology, the Fifth Medical Center of PLA General Hospital, Beijing, 100036, China; [5]Department of General Surgery, the People's Liberation Army (PLA) 305 Hospital, Beijing, 100017, China

*Correspondence: hongzhenqinhzq@163.com
#Contributed equally to this work.

Circular RNA (circ)_0000326 has been reported in bladder cancer and cervical cancer and is concerned to be involved with the development of cancerous cells. Whereas, there have been no reports concentrating on the influences of circ_0000326 in breast cancer (BC). Therefore, the latent modulatory mechanisms of circ_0000326 in BC are researched. circ_0000326 expression in BC tissues and correlative cells was evaluated via RT-qPCR, and the relevance between circ_0000326 expression and overall survival and the clinicopathological feature was also investigated. After a series of transfection, the effects of circ_0000326, microRNA-9-3p (miR-9-3p), and Yes-associated protein 1 (YAP1) in BC cell growth, invasion, and stemness were studied by CCK-8, flow cytometry, Transwell, and sphere-forming assays. The binding sites and correlation of circ_0000326, miR-9-3p, and YAP1 were certified via starBase website, luciferase reporter assay, and Pearson's χ^2 test. The in vivo experiment was evaluated by establishing a subcutaneous tumorigenesis model. High-expressed circ_0000326 in BC tissues and cells was discovered, which was connected with an undesirable prognosis. Silencing of circ_0000326 visibly inhibited MCF-7 and BT549 cell growth, invasion, stemness, meanwhile declining the protein levels of SRY-related high-mobility group box gene 2 (SOX2) and octamer binding transcription factor 4 (OCT4). miR-9-3p was a sponger of circ_0000326, which was negatively regulated by circ_0000326. Moreover, YAP1 was confirmed as a target gene of miR-9-3p. circ_0000326 affected BC cell behaviors via mediating miR-9-3p and YAP1. Furthermore, circ_0000326 silencing prohibited tumor growth of BC in vivo. The research uncovered that circ_0000326 facilitated BC development via mediating the miR-9-3p/YAP1 axis.

Key words: circular RNA_0000326; breast cancer; microRNA-9-3p; Yes-associated protein 1; tumorigenesis

The incidence of breast cancer (BC) has ranked first among female malignant tumors, which remains increasing year by year and the onset age of BC is getting younger [1]. Recently, the diagnostic level of early discovery and treatment of BC has gradually improved, which has reduced the mortality of BC to a certain extent [2]. The clinical treatments of BC involved surgical tactics, radiotherapy, chemotherapy, and traditional Chinese medicine (TCM) adjuvant therapy [3, 4]. Whereas, the characteristics of high recurrence, high metastasis, and drug resistance of BC are still urgent problems to be solved. Molecular-targeted therapy has become one of the hottest areas of various cancers [5, 6]. Therefore, an in-depth study of the mechanism of BC at the molecular level may provide effective targets for remedying and controlling the recurrence of BC.

Circular RNA (circRNA) is a class of covalently closed endogenous non-coding RNA, which possesses organization specificity and high structural stability, and is able to absorb up to 120 microRNAs (miRNAs) as competitive endogenous RNA [7, 8]. It has been proved that circRNA not only has a variety of biological functions but also can regulate gene expression at multiple levels [9]. In the research domain of BC, hsa_circ_0001982 exhibited the stimulative function in BC cell carcinogenesis via sponging miR-143 [10]. Meng et al. bore out the suppressive effect of circCCDC85A in BC progression that was mediated by miR-550a-5p and MOB kinase activator 1A (MOB1A) [11]. circ_0000326, a circRNA worth of attention, is transcribed from chromosome 11: 65,272,490-65,272,586, and has been investigated in multiple cancers, including bladder cancer and cervical cancer [12,

13]. These studies disclosed that anomalously expressed circ_0000326 was linked to cancer cells' growth, migration, and invasion. However, the influence of circ_0000326 in BC is still unclear.

At the functional level, the cancer-related miRNAs can interact with circRNAs to influence the function of downstream target genes and play a vital role in the regulation of the occurrence and development of cancers [14, 15]. The effect of miRNAs in BC has been diffusely reported, such as miR-205 [16], miR-204-5p [17], and miR-106a [18], which all participate in regulating the malignant phenotypes of BC. miR-9-3p is a significant member of miRNAs, and up-expressed miR-9-3p has been certified to accelerate cell growth of medullary thyroid carcinoma via targeting bladder cancer-associated protein (BLCAP) [19]. Moreover, Wang et al. affirmed that miR-9-3p prohibited the biological functions of gemcitabine (GEM)-treated BC cells by targeting metadherin (MTDH) [20]. Yes-associated protein 1 (YAP1) is a downstream mediator of the Hippo pathway, which is also believed to be an oncogene responsible for diversiform human cancers [21, 22]. However, whether there exists the targeted relation between miR-9-3p and YAP1 and the joint regulation of the circ_0000326 functions in BC is worth embedded exploration.

Therefore, we launched a series of experiments to study the possible mechanism of the circ_0000326-miR-9-3p-YAP1 axis in BC. The abnormal expression, mutual relation, and the effects on biological behaviors of these three factors in BC were determined. The research might provide a basis and clue for early diagnosis and targeted therapy of BC.

Patients and methods

BC tissues. The 68 BC patients (age range from 30 to 75 years old) involved in the research were from the 305 Hospital of People's Liberation Army (PLA No.305 Hospital), where the clinicopathological data were collected and BC tissues and peritumoral tissues from the above patients were gained. All participants signed informed consent forms, personally. These obtained tissues were fleetly frozen and deposited at −80 °C. All experimentation abode by the Declaration of Helsinki and was approved by the Ethics Committee of PLA No. 305 Hospital (2020-KYL-013) on March 16, 2020. In the following research, expressions of circ_0000326, miR-9-3p, and YAP1 in 68 pairs of BC tissues and peritumoral tissues were evaluated.

BC cell lines. The experimental BC cells (T47D, MCF-7, BT549, MDA-MB-231) and normal breast epithelial MCF-10A cells were obtained from the Cell Bank of the Chinese Academy of Sciences (Shanghai, China). RPMI-1640 medium (#10453001), brought from HyClone (UT, USA), was utilized for the cultivation of the above cells. After supplementation with 10% fetal bovine serum (FBS) (Gibco (Waltham, MA, USA), cells were cultured in an incubator at 37 °C with a volume fraction of 5% CO_2.

BC cell transfections. The vectors used in cell transfection such as small hairpin RNA (shRNA) targeting circ_0000326 (shRNA#1, shRNA#2, and shRNA#3) and the suited negative control (sh-NC), miR-9-3p mimic, miR-9-3p inhibitor and matched blank vectors (miR-NC and NC inhibitor), pcDNA3.1-YAP1 and pcDNA3.1 controlled vectors were designed and obtained from Dharmacon (Lafayette, CO, USA). The $2.5×10^5$ cells/well MCF-7 and BT549 cells were plated into a 6-well plate, and cultivated for 5 h at 37 °C with 5% CO_2. Subsequently, the cell transfection experiment was started by a feat of Lipofectamine 3000 reagent purchased from Sigma-Aldrich (St. Louis, MO, USA). After 48 h, transfected cells were gathered and used for the next experiments. The sequences of sh-circ_0000326 were presented as follows: 5'-GAG GTG AGT TCC CAG AGA A-3' (shRNA#1), 5'-CCG GAG CTT GGA ACA GAC T-3' (shRNA#2), 5'-CCT TTG CCG GAG CTT GGA A-3' (shRNA#3). The sequence of negative control was shown as 5'-AAG TCG GGT CAA GAG AAG C-3' (sh-NC).

Cell viability. MCF-7 and BT549 cells were transfected and grouped on the basis of the above methods, and the cell suspension of each group was prepared. Relying on the specification of Cell Counting Kit-8 (CCK-8, Absin, Shanghai, China), 100 μl of the cell suspension was replenished into the 96-well plates, along with 10 μl CCK-8 solution added at the time points of 24 h, 48 h, and 72 h. After the incubation, the absorbance was measured at 450 nm in a microplate reader (REAGEN, Shenzhen, China).

Cell apoptosis. After transfection with the above-mentioned experimental vectors, the culture medium was dislodged, the transfected cells were then washed three times with PBS (Sigma-Aldrich), and 100 μl of the cell suspension was added into a 5 ml centrifuge tube. Subsequently, PI and FITC Annexin V (BD Pharmingen, San Diego, CA, USA) with 5 μl each were mixed and added into cells and incubated for 15 min in a dark environment. 400 μl 1× Binding Buffer was supplemented and then placed in a dark room for 15 min. Flow cytometry (Guava Technologies, CA, USA) was performed for the determination of the apoptotic rates of BC cells.

Cell invasion. Transwell™ assay (Coster, Wuhan, China) was carried out for the assessment of BC cell invasion. The melted Matrigel was evenly spread on the bottom layer of the Transwell™ chamber. After the transfection, a DMEM medium without FBS was applied for the cultivation of experimental cells for 24 h, which were then fixed with 40 g/l paraformaldehyde (Solarbio, Beijing, China) for 20 min at room temperature. After 1 g/l crystal violet staining for 15 min, five different visual fields were selected for observation and the experimental cells were counted under a microscope (Nikon), the invading cells were stained purple color.

Sphere-forming assay. MCF-7 and BT549 cells were counted by flow cytometry and then placed on ultra-low adhesion 96-well plates. After transfection with sh-circ_0000326 and sh-NC, 100 μl F12 pelletizing medium

was appended into each well of the culture plates, and cells were static cultured for 14 d. Thereafter, the pellet diameter of each group was observed under an inverted microscope (Nikon, Tokyo, Japan).

Bioinformatics analysis. The circ_0000326 expression profile GSE182471 data were acquired from the Gene Expression Omnibus (GEO) database (http://www.ncbi.nlm.nih.gov/geo). The predicted binding sites of circ_0000326 and miR-9-3p, and certified whether YAP1 was a downstream target gene of miR-9-3p relying on Target Scan (http://www.targetscan.org/vert_71/).

Luciferase reporter assay. The circ_0000326 or YAP1 wild-type (circ_0000326-WT or YAP1-WT) and circ_0000326 or YAP1 mutant-type (circ_0000326-MUT or YAP1-MUT) sequences with the predicted binding sites of miR-9-3p were inserted into the luciferase reporter vectors, which were obtained from PerkinElmer (PerkinElmer, Waltham, MA, USA). Afterward, miR-9-3p mimic or miR-NC was co-transfected with aforesaid luciferase reporters by using Lipofectamine™ 3000 (Sigma-Aldrich). Forty-eight hours later, the luciferase activities were detected with the help of a Dual Luciferase Assay (#DL101-01, Vazyme, Nanjing, China). The sequences of circ_0000326-WT and circ_0000326-MUT were shown as 5'-UAU UGA AUA GAU UUC AGC UUU AU-3' and 5'-UAU UGA AUA GUA GAC UCG AAA UU-3'. The sequences of YAP1-WT and YAP1-MUT were: 5'-UAU AUC AGC AGA UUA GCU UUA G-3' and 5'-UAA AAG ACC AGA UAU CGA AUU G-3'. The sequence of miR-9-3p mimic was (sense): 5'-AUA AAG CUA GAU AAC CGA AAG U-3', (anti-sense): 5'-ACU UUC GGU UAU CUA GCU UUA U-3'. The sequence of miR-NC was shown as 5'-UUU GUA CUA CAC AAA AGU ACU G-3'.

RNase R treatment. The stability of circ_0000326 was verified via RNase R assay. The detached RNA from MCF-7 and BT549 cells was divided into two groups. RNase R (Geneseed, Guangzhou, China) was utilized to treat the above-isolated RNA (10 μg) at the density of 3 U/mg for 30 min at 37 °C. The non-treated group was regarded as a blank control. Expression of circ_0000326 was determined via RT-qPCR, subsequently.

RT-qPCR. MCF-7 and BT549 cells at the logarithmic growth stage were taken from each group, and the cell suspension was prepared after digestion with 5 g/l trypsin (Sigma-Aldrich). The total RNA from BC cells or transfected cells was isolated by utilizing RNA Isolation Kit (Qiagen, Duesseldorf, Germany). According to the PrimeScript Reverse Transcriptase Kit (Qiagen), RNA was reversely transcribed into cDNA. RT-qPCR was carried out relying on the PrimeScript™RT reagent kit (Takara, Dalian China). The reactive condition of the PCR cycle system was showcased as follows: 95 °C for 10 min, 95 °C for 15 s, 72 °C for 15 s, for a total of 30 cycles. The relative expression of circ_0000326, miR-9-3p, and YAP1 was evaluated via the $2^{-\Delta\Delta Ct}$ method. The reference of circ_0000326 and YAP1 was β-actin and U6 served as an internal reference of miR-9-3p. The sequences

of circ_0000326 were Forward: 5'-GCT TTA TGC TGG AGT AAC TG-3', Reverse: 5'-TAC AAA GTC AGA TCA GTT ATG G-3'; miR-9-3p sequences were Forward: 5'-AAG TGT CGT ATC CAG TGC AA-3', Reverse: 5'-TAT CCA GTG CGT GCG TGT C-3'; YAP1 sequences were Forward, 5'-AGA ACA ATG ACG ACC AAT AGC TC-3', Reverse, 5'-GTC GAT GGC TAG TCG TAG CAT CGAT-3'. β-actin sequences were Forward, 5'-CCC ATC TAT GAG GGT TAC GC-3', Reverse, 5'-TTT AAT GTC ACG CAC GAT TTC-3'. U6 sequences were Forward: 5'-GCT TCG GCA GCA CAT ATA CTA AAA T-3', Reverse: 5'-CGC TTC ACG AAT TTG CGT GTC AT-3'.

Western blot. After washing with ice-cold PBS, the total protein samples from transfected BC cells were extracted by the RIPA lysis buffer (Yeasen Biotechnology, Shanghai, China). After centrifugation, the supernatants were gathered and the concentrations of protein were assessed by the BCA kit (Beyotime, Shanghai, China). Following SDS-PAGE and membrane transfer, the membrane was sealed with the blocking buffer containing 50 g/l skim milk powder for 1 h. Thereafter, PVDF membranes were incubated overnight at 4 °C in a shaker with anti-SOX4 (#ab70598, 1:1000, Abcam), anti-OCT4 (#ab184665, 1:2000, Abcam), anti-YAP1 (#ab52771, 1:5000, Abcam), and anti-β-actin (#ab6276, 1:5000, Abcam). After lavation, the HRP-labeled goat anti-mouse IgG antibody (#ab205719, 1:2000, Abcam), or HRP-labeled goat anti-rabbit IgG antibody (#ab6721, 1: 2000, Abcam) were added and incubated for 1 h at ambient temperature. By using the BeyoECL Plus Kit (Beyotime), the protein blots were viewed.

RNA pull-down and RNA immunoprecipitation (RIP) assays. Based on the previous research [23], circ_0000326 biotin probe (bio-circ_0000326) and matched negative control (bio-NC) were gained from Genepharma (Shanghai, China). MCF-7 and BT549 cells were disposed of with 1% formaldehyde and scraped in 1 ml lysis buffer. After sonication and centrifugation, the supernatant was collected and cultivated with Dynabeads M-280 Streptavidin (Thermofisher, MA, USA) coating with bio-circ_0000326 or bio-NC probe. miR-9-3p enrichment was tested by RT-qPCR.

For the RIP experiment, the Magna RIP kit (Millipore, Billerica, MA, USA) was utilized. In line with the product instructions, MCF-7 and BT549 cells were dissolved with RIP buffer and then incubated with magnetic beads coated with anti-Ago2 (ab156870, 1:50, Abcam, Cambridge, UK) or anti-IgG (ab218472, 1:20, Abcam) at 4 °C overnight. The enrichment of circ_0000326 or miR-9-3p was likewise measured by RT-qPCR.

Subcutaneous tumorigenesis assay *in vivo*. The twelve BALB/c nude mice (4–5 weeks) were obtained from Beijing Vital River Laboratory Animal Technology Co., Ltd. (Beijing, China), and were fed under conventional conditions. After transfection with sh-circ_0000326 and sh-NC, 1×10^7 BT549 cells were subcutaneously injected into experimental nude mice. After this, the tumor volume and mice weight were

measured every 7 d and sustained for five weeks. After completing the statistics, mice were euthanized, and the tumors isolated from mice were photographed and weighed. After preparing paraffin tumor tissue sections, the immuno-histochemical (IHC) staining and TUNEL staining were performed, following the operating steps referred in the foregoing reports [24, 25]. All correlative animal experiments were supported by the Animal Ethics Committee of PLA No.305 Hospital.

Statistical analysis. Statistical analysis was executed depending on Prism 6.0 software (GraphPad Software Inc., CA, USA) with three repetitions. The experimental data were exhibited as mean ± standard deviation (SD). The overall survival rates were evaluated by applying Kaplan-Meier (KM)-plotter method. Pearson's χ^2 test was used for detecting the relevance of circ_0000326, miR-9-3p, and YAP1. Comparisons with multi-groups were analyzed by one-way analysis of variance (ANOVA) following Tukey's post hoc test. A statistically significant result was marked as p<0.05.

Results

circ_0000326 is up-expressed in BC, which is linked to the undesirable prognosis. To research the influences of circ_0000326 in BC, the 68 pairs of BC tissues and peritumoral tissues were gathered, and circ_0000326 expression was assessed by RT-qPCR. In comparison with pericarcinoma tissue, the circ_0000326 expression was distinctly enhanced in BC tissues (p<0.01, Figure 1A). Consistent with the RT-qPCR consequence, GSE182471 data from the GEO analytical results also discovered the highly expressed circ_0000326 in BC tissues (p<0.01, Figure 1B). Additionally, the circ_0000326 expression in BC patients > 50 years old was clearly higher than that in BC patients < 50 years old (p<0.01, Figure 1C). Furthermore, 68 cases of BC tissues were equally divided into two groups, as the high-expressed circ_0000326 (n=34) and low-expressed circ_0000326 (n=34), then the relevance between circ_0000326 expression and overall survival of BC patients was investigated. As displayed in Figure 1D, high-expressed circ_0000326 was linked to a shorter survival time hinting at a poor prognosis, whereas low-expressed circ_0000326 was related to a longer survival time, indicating a favorable prognosis (p<0.05). Moreover, the pertinence between circ_0000326 expression and clinico-pathological data of BC patients was assessed. Results uncovered that high-expressed circ_0000326 was closely related to age, TNM grade and stage, differentiation, lymph node metastasis, BC molecular type (PR) and molecular subtype [triple-negative breast cancer (TNBC) and non-TNBC] (p<0.05), but not correlated with menopausal status and size of BC patients (Table 1). Furthermore, we discovered that the expression of circ_0000326 in T47D, MCF-7, BT549, and MDA-MB-231 cells was all elevated compared with that in MCF-10A cells (p<0.05, p<0.01, Figure 1E). MCF-7

and BT549 cells were selected for the following research due to that the circ_0000326 expression was higher in these two groups than in the other groups. The circular structure of circ_0000326 was then detected via RNase R treatment. RT-qPCR analytical results uncovered that circ_0000326 was not degraded by RNase R in MCF-7 and BT549 cells (Figure 1F). Collectively, high-expressed circ_0000326 might influence the progression of BC and is related to the undesirable prognosis.

circ_0000326 silencing restrains the proliferative, invasive, and stemness abilities of BC cells. Next, the plasmids of sh-circ_0000326#1, #2, and #3 were transfected into MCF-7 and BT549 cell lines, and we discovered that the circ_0000326 expression was obviously down-regulated after transfection with the above plasmids (p<0.05 and p<0.01).

Table 1. **Correlation between circ_0000326 expression and the clinico-pathological features of 68 breast cancer patients.**

Characteristic	All cases	circ_0000326 expression		p-value
		High (n=34)	Low (n=34)	
Age (years)				0.225
<50	35	15	20	
≥50	33	19	14	
Menopause				0.807
Yes	31	16	15	
No	37	18	19	
Tumour size (cm)				0.331
<2	36	16	20	
≥2	32	18	14	
Lymph node metastasis				0.027*
Positive	39	24	15	
Negative	29	10	19	
TNM grade				0.015*
I+II	38	14	24	
III	30	20	10	
Differentiation				0.024*
Well and Moderate	25	8	17	
Poor	43	26	17	
TNM stage				0.002**
I	31	9	22	
II–III	37	25	12	
ER				0.625
Negative	38	20	18	
Positive	30	14	16	
PR				0.004**
Negative	32	22	10	
Positive	36	12	24	
HER2				0.123
Negative	55	30	25	
Positive	13	4	9	
Molecular subtype				0.020*
TNBC	26	18	8	
Non-TNBC	40	16	26	

A chi-square test was used for comparing groups between low and high circ_0000326 expression. *p<0.05, **p<0.01.
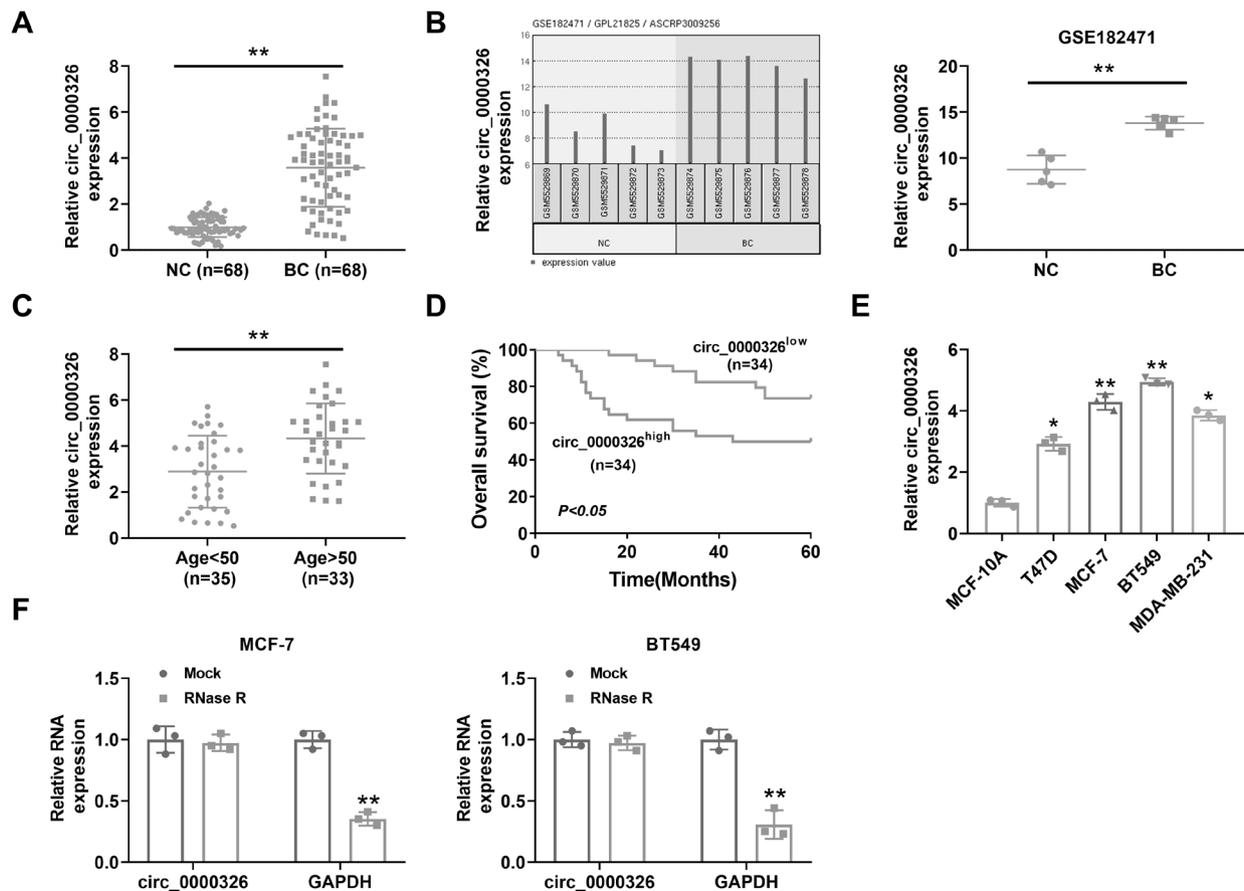
Figure 1. circ_0000326 was high-expressed in BC. (A) circ_0000326 expression in 68 pairs of BC tissues and para-carcinoma tissues was evaluated by RT-qPCR as well as **(B)** analyzed by GSE182471 from GEO data. **(C)** RT-qPCR was used to examine circ_0000326 expression in BC patients with age >50 years old (n=33) and age <50 years old (n=35). **(D)** Kaplan-Meier survival analysis was applied to determine the overall survival rate of BC patients with high-expressed circ_0000326 and low-expressed circ_0000326. **(E)** circ_0000326 expression in BC cell lines (T47D, MCF-7, BT549, and MDA-MB-231) and in normal breast epithelial MCF-10A cells was assessed by RT-qPCR. **(F)** RNase R was utilized to treat the isolated RNA from MCF-7 and BT549 cells, then circ_0000326 expression was examined via RT-qPCR. *$p<0.05$ vs. the MCF-10A cells group, **$p<0.01$ vs. NC or MCF-10A cells or the Mock group.

Moreover, sh-circ_0000326#1 transfection triggered the lowest circ_0000326 expression in MCF-7 and BT549 cells and was utilized for the subsequent experiment and marked as sh-circ_0000326 (Figure 2A). Upon the knockdown of circ_0000326 expression, cell viability and invasive ability were significantly prohibited, while the apoptotic rate was notably enhanced in MCF-7 and BT549 cells (p<0.01, Figure 2B–2D). The tumorigenesis results disclosed that the silencing of circ_0000326 obviously reduced the sphere-formation efficiency in MCF-7 and BT549 cells (p<0.01, Figure 2E). Concurrently, SOX2 and OCT4 protein levels were detected via western blot and were signally decreased by the circ_0000326 knockdown in MCF-7 and BT549 cells (p<0.01, Figure 2F). These findings manifested that circ_0000326 seemingly joined in the regulation of BC cells' swart phenotype.

circ_0000326 directly binds miR-9-3p. It has come to light that circRNAs could affect miRNA expression through the sponge function. Herein, the binding site between circ_0000326 and miR-9-3p is presented in Figure 3A, which was ascertained by the starBase database software. For further certifying the pertinence of circ_0000326 and miR-9-3p, related vectors of miR-9-3p-mimic and miR-NC were applied for transfection into MCF-7 and BT549 cells, and then the luciferase reporter assay was carried out. After transfection, the up-expressed miR-9-3p exhibited in miR-9-3p-mimic-transfected cells, indicating the successful transfection (p<0.01, Figure 3B). Moreover, miR-9-3p over-expression markedly decreased the luciferase activity of circ_0000326-WT vector as relative to the miR-NC (p<0.01), but circ_0000326-MUT vector was unchanged in both MCF-7 and BT549 cells (Figure 3C and 3D).

Following, the RNA pull-down assay disclosed that miR-9-3p enrichment was signally elevated in the bio-circ_0000326 group (p<0.01, Figure 3E). Moreover, co-immunoprecipitation results further uncovered the
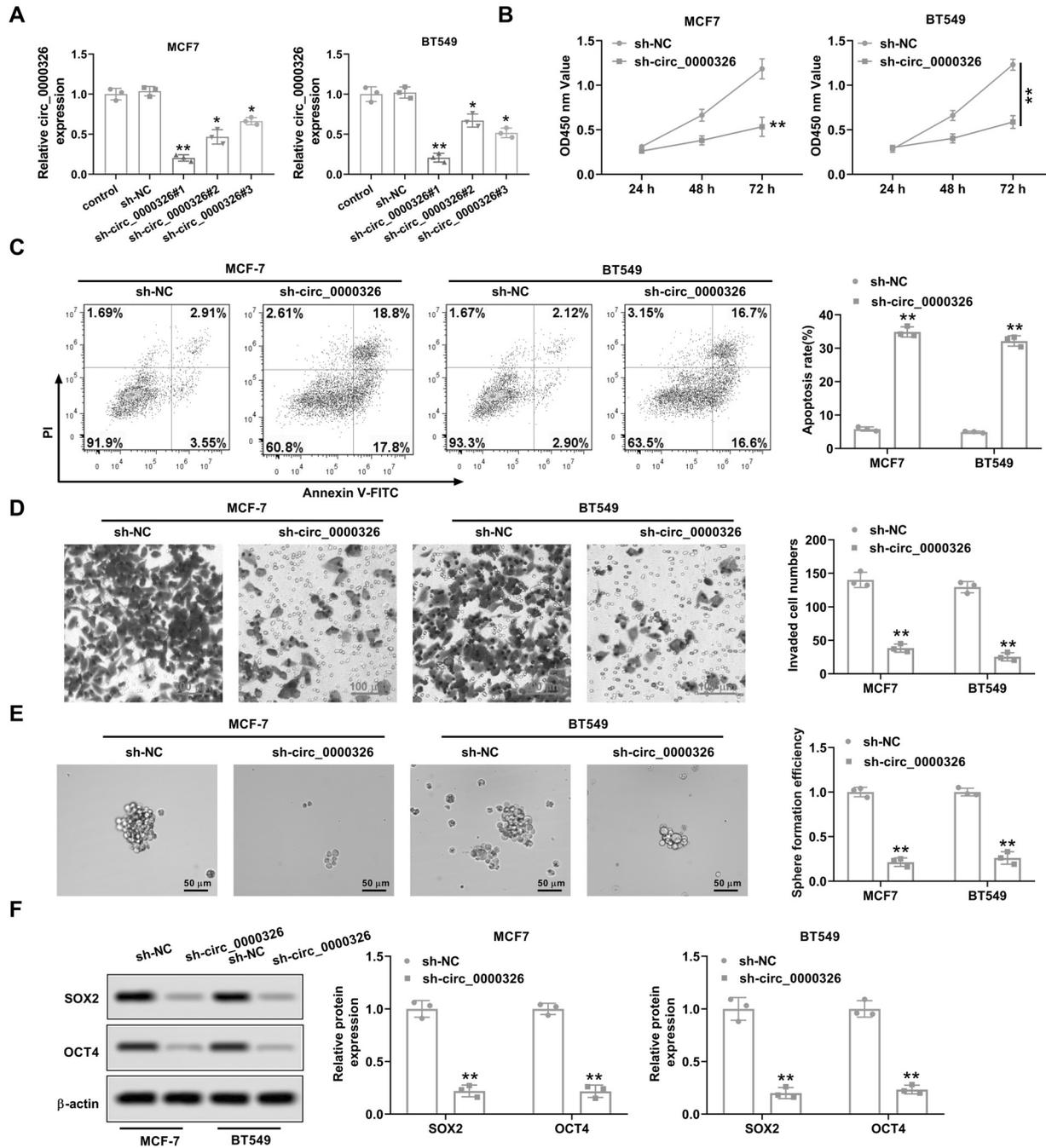
Figure 2. circ_0000326 accelerated the proliferation, invasion, and stemness of BC cells. After transfection with sh-circ_0000326 and sh-NC vectors, (A) the level of transfection in MCF-7 and BT549 cells was evaluated by RT-qPCR. Cell (B) viability, (C) apoptosis, (D) invasion, and (E) oncogenesis were researched via CCK-8, flow cytometry, Transwell, and sphere-formation assays, respectively. (F) Western blot assay was carried out for examining SOX2 and OCT4 protein levels. *p<0.05 and **p<0.01 vs. the sh-NC group.

potential relevance between circ_0000326 and miR-9-3p, which demonstrated that circ_0000326 and miR-9-3p were both enriched in the Anti-Ago2 group compared with that in the Anti-IgG group (p<0.01, Figure 3F), hinting the interaction with circ_0000326 and miR-9-3p in BC cells. Besides,

we discovered that miR-9-3p expression was obviously declined in 68 pairs of BC tissues (p<0.01, Figure 3G), and low-expressed miR-9-3p was accompanied by an undesirable prognosis (p<0.05, Figure 3H). The clinicopathological information illustrated that miR-9-3p expression was implicated
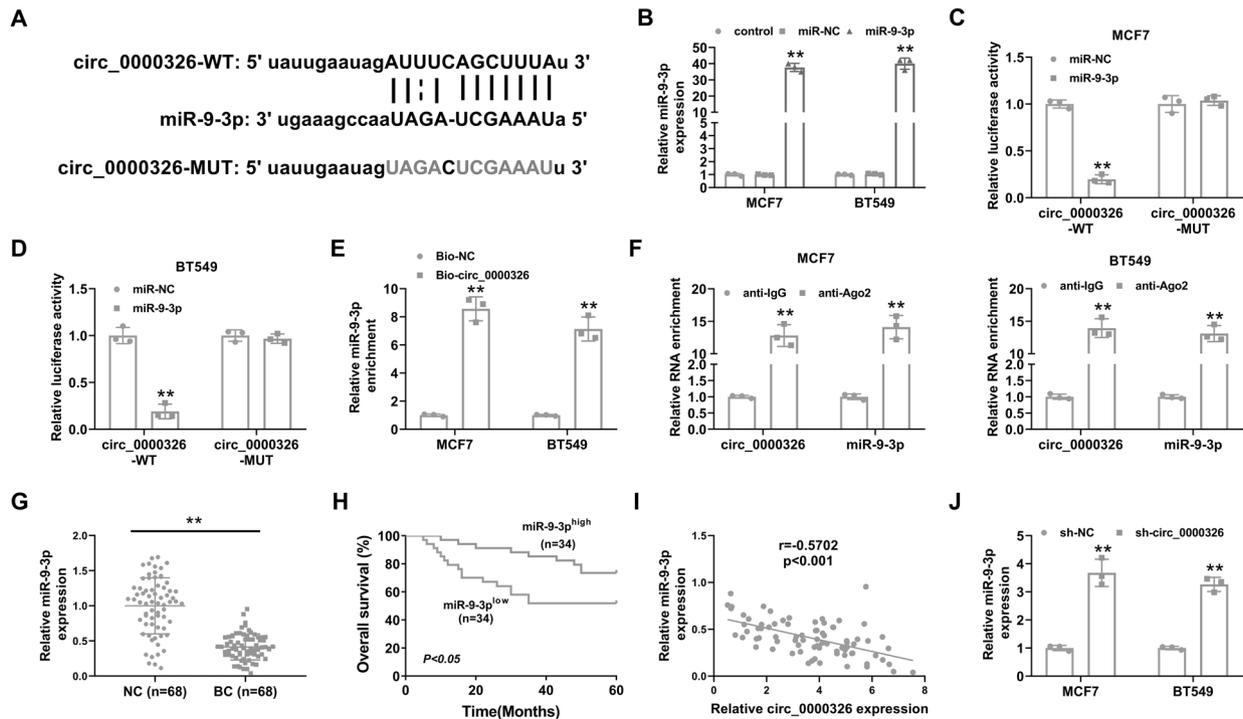
Figure 3. circ_0000326 bound with miR-9-3p. (A) The binding sites between circ_0000326 and miR-9-3p were forecasted by the starBase website. After miR-9-3p-mimic and miR-NC vectors transfection, **(B)** the transfection efficiency was examined via RT-qPCR. **(C and D)** The luciferase reporter assay was performed to further certify the prediction in MCF-7 and BT549 cells. **(E)** RNA pull-down and **(F)** co-immunoprecipitation assays were utilized to investigate the potential relevance between circ_0000326 and miR-9-3p. **(G)** Relative miR-9-3p expression in 68 pairs of BC tissues and para-carcinoma tissues was studied using RT-qPCR. **(H)** The overall survival rates of BC patients with high-expressed miR-9-3p and low-expressed miR-9-3p were assessed via Kaplan-Meier survival analysis. **(I)** The correlation between circ_0000326 and miR-9-3p was detected using Pearson's χ^2 test. **(J)** miR-9-3p expression in sh-circ_0000326 and sh-NC transfected cells was studied by RT-qPCR. **p<0.01 vs. miR-NC, Bio-NC, anti-IgG, or sh-NC.

with the TNM stage and lymph node metastasis (p<0.05, Table 2). Relevance analysis discovered that miR-9-3p was negatively correlated with circ_0000326 (p<0.001, Figure 3I), moreover, it was up-regulated in sh-circ_0000326-transfected BC cells (p<0.01, Figure 3J). Summarily, circ_0000326 could sponge miR-9-3p in BC cells.

miR-9-3p negatively mediates the YAP1 protein level. The online database was used to survey the regulatory mechanism of miR-9-3p in BC cells. YAP1 was predicated as a downstream targeted gene of miR-9-3p, which binding site is displayed in Figure 4A. The luciferase activity of YAP1-WT showcased in Figure 4B was notably reduced in miR-9-3p-mimic-transfected cells (p<0.01). However, there was no evident imparity in the YAP1-MUT group. Western blot experiment revealed that the overexpression of miR-9-3p triggered an obviously reduced tendency of YAP1 protein level in MCF-7 and BT549 cells (p<0.01, Figure 4C). For further evaluation of the relationship between miR-9-3p and YAP1, the miR-9-3p inhibitor vector was utilized to transfect into MCF-7 and BT549 cells in order to decrease miR-9-3p expression. The successful transfection is exhibited in Figure 4D (p<0.01). YAP1 protein level was clearly lowered by circ_0000326 silencing (p<0.01), while the result

Table 2. Correlation between miR-9-3p expression and the clinicopathological features of 68 breast cancer patients.

Characteristic	All cases	miR-9-3p expression		p-value
		High (n=34)	Low (n=34)	
Age (years)				0.089
<50	35	21	14	
≥50	33	13	20	
Menopause				0.465
Yes	31	14	17	
No	37	20	17	
Tumour size (cm)				0.627
<2	36	19	17	
≥2	32	15	17	
Lymph node metastasis				0.007**
Positive	39	14	25	
Negative	29	20	9	
TNM grade				0.006**
I+II	38	26	12	
III	30	8	22	
Differentiation				0.451
Well and Moderate	25	11	14	
Poor	43	23	20	

A chi-square test was used for comparing groups between low and high miR-9-3p expression. **p <0.01.

was reversed following the transfection of miR-9-3p inhibitor (p<0.05, Figure 4E). Subsequently, the up-expressed YAP1 was exhibited in 68 BC tissues (p<0.01, Figure 4F), which was related to a poor prognosis (p<0.05, Figure 4G) and likewise correlated with the TNM stage and lymph node metastasis (p<0.05, Table 3). Correlation analysis showcased that YAP1 was negatively associated with miR-9-3p expression, but was positively linked with circ_0000326 expression (p<0.001, Figure 4H and 4I). The above data demonstrated that YAP1 might be a target gene of miR-9-3p, which is negatively regulated by miR-9-3p in BC cells.

circ_0000326 promotes the malignant progression of BC cells by modulating the miR-9-3p/YAP1 axis. To uncover the function of YAP1, the overexpressed vector of YAP1 was transfected into BC cells. We noticed that YAP1 overexpression significantly elevated YAP1 protein level in MCF-7 and BT549 cells (p<0.01, Figure 5A). After a series of transfection, BC cell growth and invasion were further evaluated. The results disclosed that circ_0000326 silencing induced inhibitory or accelerative functions in cell viability,

invasion, and apoptosis were obviously overturned in BC cells after co-transfection with miR-9-3p inhibitor or YAP1 overexpressing vectors (p<0.05, p<0.01, Figures 5B–5D). Similarly, the depressed levels of SOX2 and OCT4 triggered by circ_0000326 silencing were also reversed by miR-9-3p inhibition or YAP1 overexpression in BC cells (p<0.05, p<0.01, Figure 5E). These results unearthed that miR-9-3p/YAP1 axis might join in regulating the influence of circ_0000326 in the malignant progression of BC cells.

circ_0000326 silencing restrains tumor growth of BC *in vivo*. For deeper certification of the effect of circ_0000326 in BC, the subcutaneous tumorigenesis experiment in nude mice was performed. As emerged in Figures 6A–6D, circ_0000326 silencing dramatically astricted tumor growth, restrained tumor volume, and lowered tumor weight (p<0.01), whereas did not make an impact on mice weight. IHC detective results revealed that protein levels of YAP1, SOX2, and OCT4 were all limited by circ_0000326 silencing (p<0.01, Figure 6E). Beyond that, the TUNEL staining assay results showcased that the positive-TUNEL cells in the sh-circ_0000326-transfected
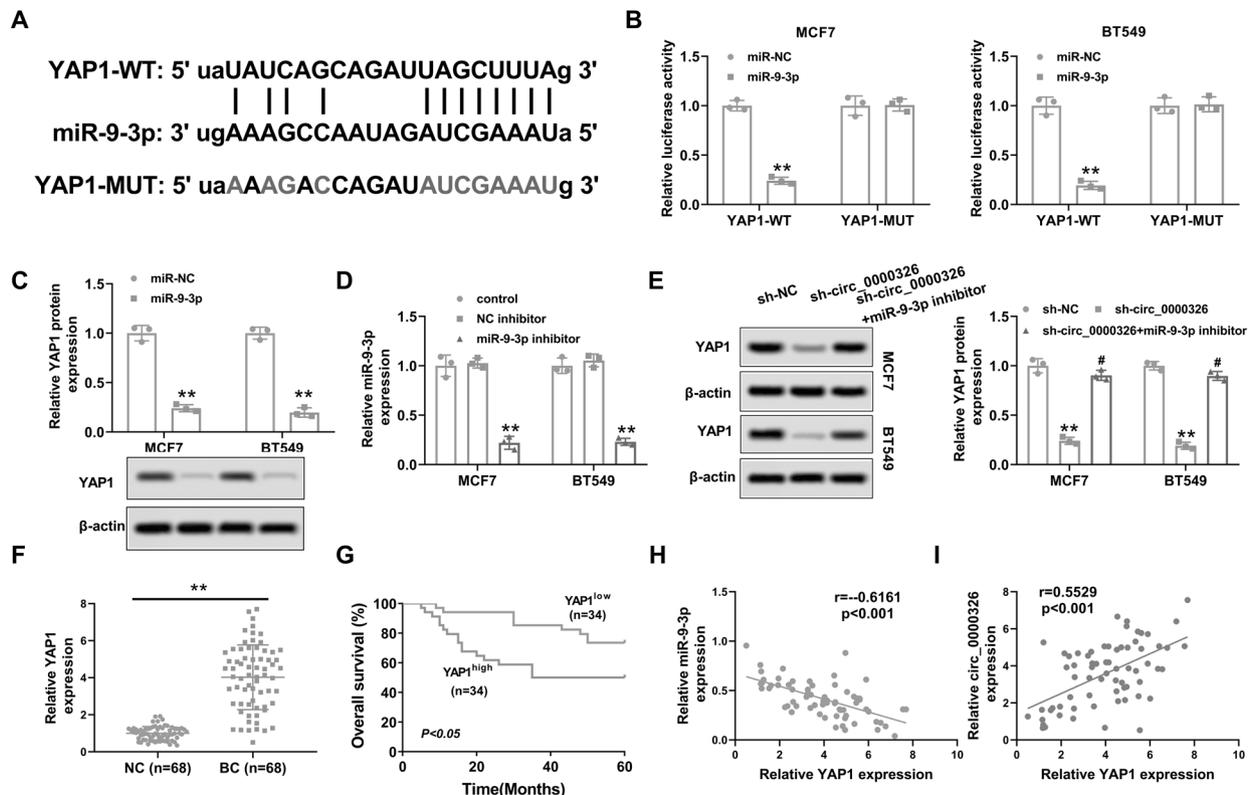

Figure 4. YAP1 was a target mRNA of miR-9-3p. (A) The starBase website was utilized to predict the binding sites between miR-9-3p and YAP1. (B) The luciferase activities of YAP1-WT and YAP1-MUT in miR-9-3p-mimic and miR-NC transfected cells were explored by the luciferase reporter assay. (C) The protein level of YAP1 in miR-9-3p-mimic and miR-NC transfected cells was determined by western blot. (D) After transfection with miR-9-3p inhibitor and NC inhibitor, the level of transfection was assessed by RT-qPCR. (E) After co-transfection with sh-circ_0000326 and miR-9-3p inhibitor, protein levels of YAP1 in MCF-7 and BT549 cells were examined by western blot. (F) YAP1 expression in 68 pairs of BC tissues and para-carcinoma tissues was researched by RT-qPCR. (G) The overall survival rates of BC patients with high-expressed YAP1 and low-expressed YAP1 were detected via Kaplan-Meier survival analysis. (H and I) The correlation among circ_0000326, miR-9-3p, and YAP1 was detected by Pearson's χ^2 test. **p<0.01 vs. miR-NC, NC inhibitor, or NC tissues; #p<0.05 vs. sh-circ_0000326.
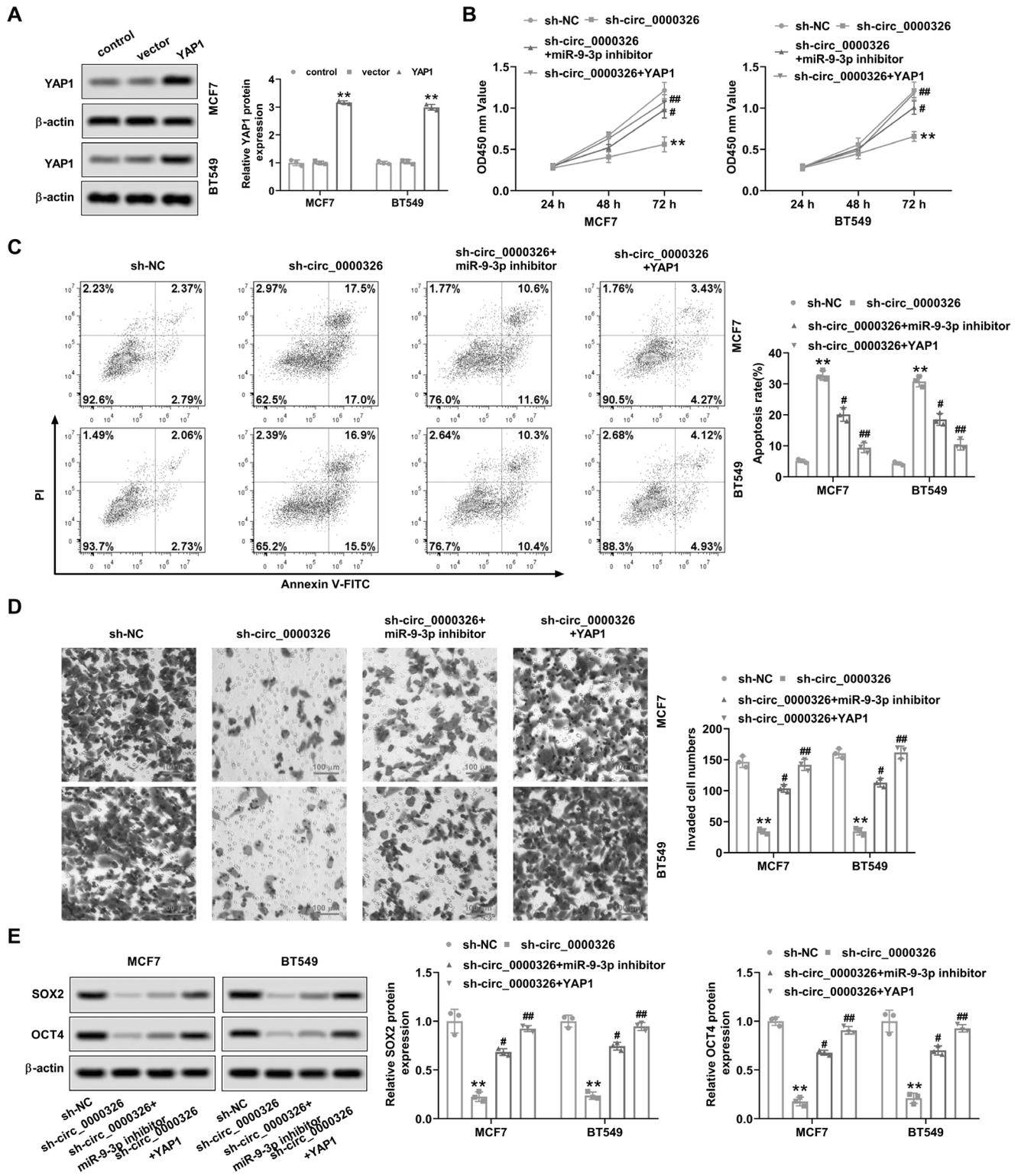
Figure 5 circ_0000326 mediated the malignant progression by the miR-9-3p/YAP1 axis. (A) After transfection with overexpressed YAP1 and corresponding control vectors, protein levels of YAP1 were determined by western blot. After co-transfection with sh-circ_0000326 and miR-9-3p inhibitor or YAP1 overexpressed vector, (B) OD450 value of cell viability, (C) cell apoptosis, and (D) cell invasion were studied by CCK-8, flow cytometry, and Transwell methods. (E) Protein levels of SOX2 and OCT4 were examined by western blot assay. **p<0.01 vs. the sh-NC group, #p<0.05, ##p<0.01 vs. sh-circ_0000326.

Table 3. Correlation between YAP1 expression and the clinicopathological features of 68 breast cancer patients.

Characteristic	All cases	YAP1 expression		p-value
		High (n=34)	Low (n=34)	
Age (years)				0.808
<50	35	17	18	
≥50	33	17	16	
Menopause				0.223
Yes	31	18	13	
No	37	16	21	
Tumour size (cm)				0.145
<2	36	21	15	
≥2	32	13	19	
Lymph node metastasis				0.0001***
Positive	39	28	11	
Negative	29	6	23	
TNM grade				0.003**
I+II	38	13	25	
III	30	21	9	
Differentiation				0.078
Well and Moderate	25	9	16	
Poor	43	25	18	

A chi-square test was used for comparing groups between low and high YAP1 expression. **$p<0.01$, ***$p<0.001$.

group were obviously increased relative to that in the sh-NC-transfected group ($p<0.01$, Figure 6F). Finally, circ_0000326, miR-9-3p, and YAP1 expressions in subcutaneous tumor tissues of BT549 cells were detected by RT-qPCR. Results displayed that down-regulated circ_0000326 enhanced the miR-9-3p expression but reduced the YAP1 expression ($p<0.01$, Figure 6G). All these consequences made clear that the silencing of circ_0000326 could inhibit tumor growth of BC *in vivo*.

Discussion

From miRNAs, lncRNAs, to circRNAs, the complex biological functions of non-coding RNA (ncRNA) are increasingly being studied in tumors and are considered as molecular markers for tumor diagnosis and prognosis assessment [26]. As an emerging regulatory molecule, circRNA is involved in BC proliferation, invasion, metastasis, and chemotherapeutic resistance [27, 28]. Nonetheless, the functions of circ_0000326 in BC have not been explored yet. In the current research, the up-expressed circ_0000326 was discovered in BC tissues and cells, which was implicated with a poor prognosis. Moreover, the silencing of circ_0000326 suppressed malignant behaviors of BC cells via mediating the miR-9-3p/YAP1 expression. Furthermore, the inhibitory influence of circ_0000326 was also explained in tumor growth of BC *in vivo*.

With the deepening of research, the significant position of circRNAs in various kinds of cancers has been highlighted [29]. As a vital circRNA, circ_0000326 has been probed in

the cancer field [30]. The up-regulated circ_0000326 in lung adenocarcinoma was reported by Xu et al. [31] and was certified to be connected with the pathological staging of the tumor. Likewise, we also noticed that circ_0000326 expression was enhanced in BC tissues and cells, and was closely related to the TNM stage, lymph node metastasis, and differentiation. The evidences for promoting cancer of circ_0000326 have been confirmed by Chen et al. [12] and Wang et al. [13]. Concretely, circ_0000326 facilitated bladder cancer and cervical cancer cells' proliferation, migration, and invasion. Herein, circ_0000326 similarly accelerated cell growth (proliferation and apoptosis), invasion, and stemness in MCF-7 and BT549 cells, which was certified to serve as a tumor promoter of BC.

CircRNA is able to sponge miRNA, prohibiting the activity of miRNA, thus affecting the regulation of miRNA on downstream proto-oncogenes or tumor suppressor genes, meanwhile influencing the biological behaviors of cancer cells, including proliferation, apoptosis, and metastasis [32, 33]. On the basis of the bioinformatics analysis, we discovered that circ_0000326 could interact with miR-9-3p, which was further verified by the luciferase reporter assay. A recent research showcased that circVMA21 mediated the miR-9-3p/SMG1 inflammation axis to improve sepsis-related acute kidney injury [34]. Also, circPLEKHM3 played a tumor suppressor in ovarian cancer by mediating miR-9 expression [35]. Moreover, Higashi et al. showcased that miR-9-3p prohibited hepatocellular carcinoma (HCC) cells' proliferative and invasive abilities by targeting the PDZ-binding motif (TAZ) [36]. Besides, miR-9-3p affected BC cell behaviors by targeting the β_1 integrin gene (*ITGB1*) and regulating MEK inhibition [37]. But, whether circ_0000326 showcased the stimulative effect on BC progression via regulating miR-9-3p is still not a concern. Moreover, it is worth exploring whether there exists a gene-targeted relationship with miR-9-3p to participate in modulating the effect of circ_0000326 on BC cells. Herein, the study uncovered that miR-9-3p could directly sponge circ_0000326, moreover, which negatively regulated YAP1 expression. The findings hinted that miR-9-3p targeted YAP1 to influence the malignant phenotypes of BC triggered by circ_0000326.

As a crucial effector of the Hippo signal pathway, YAP1 is qualified for regulating cell proliferation and tumorigenesis [38]. The function as an oncogene of YAP1 has been broadly ascertained in a nice bit of cancer forms, including BC [39, 40]. Research from Wang et al. attested that YAP1 was involved in facilitating the tumorigenesis of BC induced by circ_0005273 [41]. Additionally, circ_0023404 exhibited an oncogenic function in cervical cancer by mediating the miR-136/YAP pathway [42]. Beyond that, circ-HIPK3 regulated YAP1 expression to accelerate the progression of oral squamous cell carcinoma by sponging miR-381-3p [43]. These studies hinted that the circRNA-miRNA-mRNA axis exhibited momentous function in tumor development. In this research, we discovered that circ_0000326 sponged
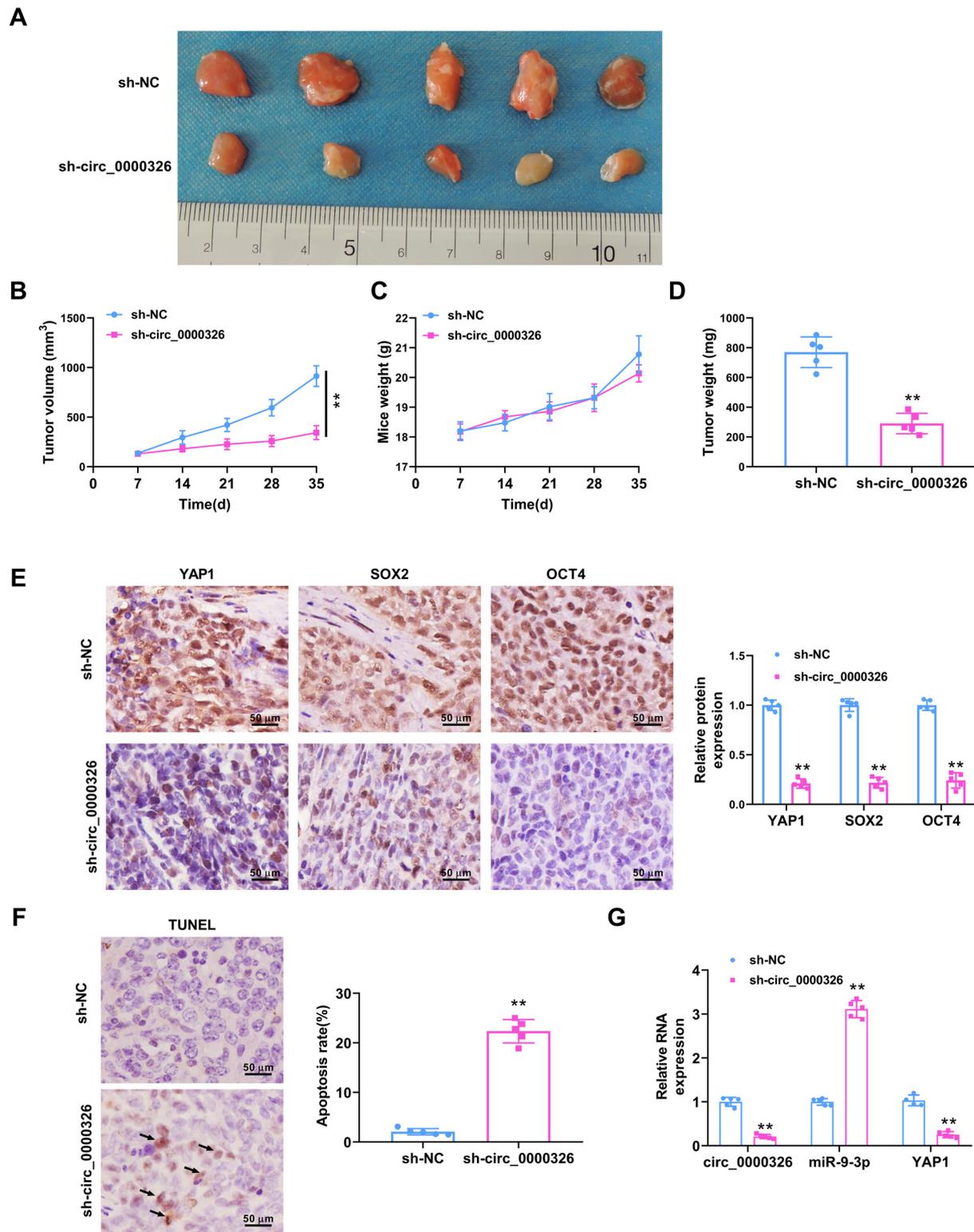
Figure 6 circ_0000326 promoted tumor growth of BC *in vivo*. After transfection with sh-circ_0000326 and sh-NC in BT549 cells, the animal model of the subcutaneous tumorigenesis was constructed. (A) The tumor size, (B) tumor volume, (C) mice weight, and (D) tumor weight were measured. (E) Relative protein levels of YAP1, SOX2, and OCT4 were studied by the IHC assay. (F) Apoptosis rates in sh-circ_0000326 and sh-NC transfected BT549 cells were detected by TUNEL staining. (G) Relative RNA expressions of circ_0000326, miR-9-3p, and YAP1 were determined by RT-qPCR. **p<0.01 vs. the sh-NC group.

miR-9-3p to modulate the endogenous expression of YAP1, thus influencing BC progression *in vitro* and *in vivo*.

Conclusion. To sum up, the research furnished evidence that circ_0000326 accelerated the progression of BC through sponging miR-9-3p and regulating YAP1 expression. The circ_0000326-miR-9-3p-YAP1 axis might be important for early screening of BC, providing endless potential for the development of BC biomarker and therapeutic strategies. circ_0000326 is expected to be a novel target for accurate diagnosis and treatment of BC. However, the effect of circ_0000326 focusing on BC cells' metastasis and related signaling pathway is still defective. Following, the study will expand clinical samples to further explore the mechanism of circ_0000326 in BC.

References

[1] RYSER MD, LANGE J, INOUE LY, O'MEARA ES, GARD C et al. Estimation of breast cancer overdiagnosis in a US breast screening cohort. Ann Int Med 2022; 175: 471–478. https://doi.org/10.7326/M21-3577

[2] ALLUGUNTI VR. Breast cancer detection based on thermographic images using machine learning and deep learning algorithms. Int J Engineering Comp Sci 2022; 4: 49–56. https://doi.org/10.33545/26633582.2022.v4.i1a.68

[3] HE L, WANG X, LIU X, JIA Y, ZHAO W et al. Analysis of Clinical Characteristics, Treatment, and Prognostic Factors of 106 Breast Cancer Patients With Solitary Pulmonary Nodules. Front Surg 2022; 9: 843913. https://doi.org/10.3389/fsurg.2022.843913

[4] POO CL, DEWADAS HD, NG FL, FOO CN, LIM YM. Effect of traditional Chinese medicine on musculoskeletal symptoms in breast cancer: a systematic review and meta-analysis. J Pain Symptom Manage 2021; 62: 159–173. https://doi.org/10.1016/j.jpainsymman.2020.11.024

[5] LEE YT, TAN YJ, OON CE. Oon, Molecular targeted therapy: Treating cancer with specificity. Eur J Pharmacol 2018; 834: 188–196. https://doi.org/10.1016/j.ejphar.2018.07.034

[6] IMYANITOV EN, IYEVLEVA AG, LEVCHENKO EV. Molecular testing and targeted therapy for non-small cell lung cancer: current status and perspectives. Crit Rev Oncol Hematol 2021; 157: 103194. https://doi.org/10.1016/j.critrevonc.2020.103194

[7] NIELSEN AF, BINDEREIF A, BOZZONI I, HANAN M, HANSEN TB et al. Best practice standards for circular RNA research. Nat Methods 2022; 19: 1–13. https://doi.org/10.1038/s41592-022-01487-2

[8] WANG Y, WU C, DU Y, LI Z, LI M et al. Expanding uncapped translation and emerging function of circular RNA in carcinomas and noncarcinomas. Mol Cancer 2022; 21: 13. https://doi.org/10.1186/s12943-021-01484-7

[9] CHENG D, WANG J, DONG Z, LI X. Cancer-related circular RNA: diverse biological functions. Cancer Cell Int 2021; 21: 11. dio: 10.1186/s12935-020-01703-z

[10] TANG YY, ZHAO P, ZOU TN, DUAN JJ, ZHI R et al. Circular RNA hsa_circ_0001982 promotes breast cancer cell carcinogenesis through decreasing miR-143. DNA Cell Biol 2017; 36: 901–908. https://doi.org/10.1089/dna.2017.3862

[11] MENG L, CHANG S, SANG Y, DING P, WANG L et al. Circular RNA circCCDC85A inhibits breast cancer progression via acting as a miR-550a-5p sponge to enhance MOB1A expression. Breast Cancer Res 2022; 24: 1. https://doi.org/10.1186/s13058-021-01497-6

[12] CHEN Y, WANG D, SHU T, SUN K, ZHAO J et al. Circular RNA_0000326 promotes bladder cancer progression via microRNA-338-3p/ETS Proto-Oncogene 1/phosphoinositide-3 kinase/Akt pathway. Bioengineered 2021; 12: 11410–11422. https://doi.org/10.1080/21655979.2021.2008738

[13] WANG Z, REN C, YANG L, ZHANG X, LIU J et al. Silencing of circular RNA_0000326 inhibits cervical cancer cell proliferation, migration and invasion by boosting microRNA-338-3p-dependent down-regulation of CDK4. Aging (Albany NY) 2021; 13: 9119–9134. https://doi.org/10.18632/aging.103711

[14] LIANG ZZ, GUO C, ZOU MM, MENG P, ZHANG TT. Zhang, circRNA-miRNA-mRNA regulatory network in human lung cancer: an update. Cancer Cell Int 2020; 20: 173. https://doi.org/10.1186/s12935-020-01245-4

[15] ZHANG M, BAI X, ZENG X, LIU J, LIU F et al. circRNA-miRNA-mRNA in breast cancer. Clin Chim Acta 2021; 523: 120–130. https://doi.org/10.1016/j.cca.2021.09.013

[16] ZHAO Y, JIN LJ, ZHANG XY. Exosomal miRNA-205 promotes breast cancer chemoresistance and tumorigenesis through E2F1. Aging (Albany NY) 2021; 13: 18498–18514. https://doi.org/10.18632/aging.203298

[17] HONG BS, RYU HS, KIM N, KIM J, LEE E et al. Tumor suppressor miRNA-204-5p regulates growth, metastasis, and immune microenvironment remodeling in breast cancer. Cancer Res 2019; 79: 1520–1534. https://doi.org/10.1158/0008-5472.CAN-18-0891

[18] YOU F, LUAN H, SUN D, CUI T, DING P et al. miRNA-106a promotes breast cancer cell proliferation, clonogenicity, migration, and invasion through inhibiting apoptosis and chemosensitivity. DNA Cell Biol 2019; 38: 198–207. https://doi.org/10.1089/dna.2018.4282

[19] Chen Y, Zhang S, Zhao R, Zhao Q, Zhang T. Upregulated miR-9-3p promotes cell growth and inhibits apoptosis in medullary thyroid carcinoma by targeting BLCAP. Oncol Res 2017; 25: 1215–1222. https://doi.org/10.3727/096504016X14791715355957

[20] WANG Y, DONG L, WAN F, CHEN F, LIU D et al. MiR-9-3p regulates the biological functions and drug resistance of gemcitabine-treated breast cancer cells and affects tumor growth through targeting MTDH. Cell Death Dis 2021; 12: 861. https://doi.org/10.1038/s41419-021-04145-1

[21] LI M, LU J, ZHANG F, LI H, ZHANG B et al. Yes-associated protein 1 (YAP1) promotes human gallbladder tumor growth via activation of the AXL/MAPK pathway. Cancer Lett 2014; 355: 201–209. https://doi.org/10.1016/j.canlet.2014.08.036

[22] KANG W, TONG JHM, CHAN AWH, LEE TL, LUNG RWM et al. Yes-Associated Protein 1 Exhibits Oncogenic Property in Gastric Cancer and Its Nuclear Accumulation Associates with Poor Prognosis YAP1 Exhibits Oncogenic Property in Gastric Cancer. Clin Cancer Res 2011; 17: 2130–2139. https://doi.org/10.1158/1078-0432.CCR-10-2467

[23] DING Y, WANG M, YANG J. Circular RNA midline-1 (circMID1) promotes proliferation, migration, invasion and glycolysis in prostate cancer. Bioengineered 2022; 13: 6293–6308. https://doi.org/10.1080/21655979.2022.2037367

[24] LIANG G, LING Y, MEHRPOUR M, SAW PE, LIU Z et al. Autophagy-associated circRNA circCDYL augments autophagy and promotes breast cancer progression. Mol Cancer 2020; 19: 65. https://doi.org/10.1186/s12943-020-01152-2

[25] CHEN W, WANG H, FENG J, CHEN L. Overexpression of circRNA circUCK2 attenuates cell apoptosis in cerebral ischemia-reperfusion injury via miR-125b-5p/GDF11 signaling. Mol Ther Nucleic Acids 2020; 22: 673–683. https://doi.org/10.1016/j.omtn.2020.09.032

[26] TORNESELLO ML, FARAONIO R, BUONAGURO L, ANNUNZIATA C, STARITA N et al. The role of microRNAs, long non-coding RNAs, and circular RNAs in cervical cancer. Front Oncol 2020; 10: 150. https://doi.org/10.3389/fonc.2020.00150

[27] LI Z, CHEN Z, HU G, JIANG Y. Roles of circular RNA in breast cancer: present and future. Am J Transl Res 2019; 11: 3945–3954.

[28] JAHANI S, NAZERI E, MAJIDZADEH-A K, JAHANI M, ESMAEILI R. Circular RNA; a new biomarker for breast cancer: a systematic review. J Cell Physiol 2020; 235: 5501–5510. https://doi.org/10.1002/jcp.29558

[29] CHEN L, SHAN G. CircRNA in cancer: Fundamental mechanism and clinical potential. Cancer Lett 2021; 505: 49–57. https://doi.org/10.1016/j.canlet.2021.02.004

[30] MOGHBELI M. Molecular interactions of miR-338 during tumor progression and metastasis. Cell Mol Biol Lett 2021; 26: 13. https://doi.org/10.1186/s11658-021-00257-w

[31] XU Y, YU J, HUANG Z, FU B, TAO Y et al. Circular RNA hsa_circ_0000326 acts as a miR-338-3p sponge to facilitate lung adenocarcinoma progression. J Exp Clin Cancer Res 2020; 39: 57. https://doi.org/10.1186/s13046-020-01556-4

[32] YANG SJ, WANG DD, ZHOU SY, ZHANG Q, WANG JY et al. Identification of circRNA–miRNA networks for exploring an underlying prognosis strategy for breast cancer. Epigenomics 2020; 12: 101–125. https://doi.org/10.2217/epi-2019-0058

[33] CHENG J, ZHUO H, XU M, WANG L, XU H et al. Regulatory network of circRNA–miRNA–mRNA contributes to the histological classification and disease progression in gastric cancer. J Transl Med 2018; 16: 216. https://doi.org/10.1186/s12967-018-1582-8

[34] SHI Y, SUN CF, GE WH, DU YP, HU NB. Circular RNA VMA21 ameliorates sepsis-associated acute kidney injury by regulating miR-9-3p/SMG1/inflammation axis and oxidative stress. J Cell Mol Med 2020; 24: 11397–11408. https://doi.org/10.1111/jcmm.15741

[35] ZHANG L, ZHOU Q, QIU Q, HOU L, WU M et al. Circ-PLEKHM3 acts as a tumor suppressor through regulation of the miR-9/BRCA1/DNAJB6/KLF4/AKT1 axis in ovarian cancer. Mol Cancer 2019; 18: 144. https://doi.org/10.1186/s12943-019-1080-5

[36] HIGASHI T, HAYASHI H, ISHIMOTO T, TAKEYAMA H, KAIDA T et al. miR-9-3p plays a tumour-suppressor role by targeting TAZ (WWTR1) in hepatocellular carcinoma cells. Br J Cancer 2015; 113: 252–258. https://doi.org/10.1038/bjc.2015.170

[37] ZAWISTOWSKI JS, NAKAMURA K, PARKER JS, GRANGER DA, GOLITZ BT et al. MicroRNA 9-3p targets β1 integrin to sensitize claudin-low breast cancer cells to MEK inhibition. Mol Cell Biol 2013; 33: 2260–2274. https://doi.org/10.1128/MCB.00269-13

[38] GHAFOURI-FARD S, HUSSEN BM, TAHERI M, AYATOLLAHI SA. Emerging role of circular RNAs in breast cancer. Pathol Res Pract 2021; 223: 153496. https://doi.org/10.1016/j.prp.2021.153496

[39] ZHANG Y, WANG Y, JI H, DING J, WANG K. The interplay between noncoding RNA and YAP/TAZ signaling in cancers: molecular functions and mechanisms. J Exp Clin Cancer Res 2022; 41: 202. https://doi.org/10.1186/s13046-022-02403-4

[40] ZHOU Y, LIU X, LAN J, WAN Y, ZHU X. Circular RNA circRPPH1 promotes triple-negative breast cancer progression via the miR-556-5p/YAP1 axis. Am J Transl Res 2020; 12: 6220–6234.

[41] WANG X, JI C, HU J, DENG X, ZHENG W et al. Hsa_circ_0005273 facilitates breast cancer tumorigenesis by regulating YAP1-hippo signaling pathway. J Exp Clin Cancer Res 2021; 40: 29. https://doi.org/10.1186/s13046-021-01830-z

[42] ZHANG J, ZHAO X, ZHANG J, ZHENG X, LI F. Circular RNA hsa_circ_0023404 exerts an oncogenic role in cervical cancer through regulating miR-136/TFCP2/YAP pathway. Biochem Biophys Res Commun 2018; 501: 428–433. https://doi.org/10.1016/j.bbrc.2018.05.006

[43] BI L, ZHANG C, YAO Y, HE Z. Circ-HIPK3 regulates YAP1 expression by sponging miR-381-3p to promote oral squamous cell carcinoma development. J Biosci 2021; 46: 20. https://doi.org/10.1007/s12038-021-00142-w